Neuroscience 284 (2015) 470–482

THE PRE- AND POST-SOMATIC SEGMENTS OF THE HUMAN TYPE I SPIRAL GANGLION NEURONS – STRUCTURAL AND FUNCTIONAL CONSIDERATIONS RELATED TO COCHLEAR IMPLANTATION

W. LIU, [a,b] **F. EDIN,** [a,b] **F. ATTURO,** [a,c] **G. RIEGER,** [d] **H. LÖWENHEIM,** [e†] **P. SENN,** [f,g] **M. BLUMER,** [h] **A. SCHROTT-FISCHER,** [d*] **H. RASK-ANDERSEN** [a,b*] **AND R. GLUECKERT** [d]

[a] *Department of Surgical Sciences, Head and Neck Surgery, Section of Otolaryngology, Uppsala University Hospital, SE-751 85 Uppsala, Sweden*

[b] *Department of Otolaryngology, Uppsala University Hospital, SE-751 85 Uppsala, Sweden*

[c] *Department of Neurology, Mental Health and Sensory Organs, Otorhinolaryngologic Unit, Medicine and Psychology, Sapienza, Rome, Italy*

[d] *Department of Otolaryngology, Medical University of Innsbruck, Anichstrasse 35, A-6020 Innsbruck, Austria*

[e] *Department of Otorhinolaryngology-Head & Neck Surgery, European Medical School, University of Oldenburg, Steinweg 13-17, 26122 Oldenburg, Germany*

[f] *University Department of ORL, Head & Neck Surgery, Inselspital and Department of Clinical Research, University of Bern, Switzerland*

[g] *University Department of ORL, Head & Neck Surgery, HUG, Geneva, Switzerland*

[h] *Department of Anatomy, Histology and Embryology, Division of Clinical and Functional Anatomy, Medical University of Innsbruck, Müllerstrasse 59, 6020 Innsbruck, Austria*

Abstract—Human auditory nerve afferents consist of two separate systems; one is represented by the large type I cells innervating the inner hair cells and the other one by the small type II cells innervating the outer hair cells. Type I spiral ganglion neurons (SGNs) constitute 96% of the afferent nerve population and, in contrast to other mammals, their soma and pre- and post-somatic segments are unmyelinated. Type II nerve soma and fibers are unmyelinated. Histopathology and clinical experience imply that human SGNs can persist electrically excitable without dendrites, thus lacking connection to the organ of Corti. The biological background to this phenomenon remains elusive. We analyzed the pre- and post-somatic segments of the type I human SGNs using immunohistochemistry and transmission electron microscopy (TEM) in normal and pathological conditions. These segments were found surrounded by non-myelinated Schwann cells (NMSCs) showing strong intracellular expression of laminin-β2/collagen IV. These cells also bordered the perikaryal entry zone and disclosed surface rugosities outlined by a folded basement membrane (BM) expressing laminin-β2 and collagen IV. It is presumed that human large SGNs are demarcated by three cell categories: (a) myelinated Schwann cells, (b) NMSCs and (c) satellite glial cells (SGCs). Their BMs express laminin-β2/collagen IV and reaches the BM of the sensory epithelium at the habenula perforata. We speculate that the NMSCs protect SGNs from further degeneration following dendrite loss. It may give further explanation why SGNs can persist as electrically excitable monopolar cells even after long-time deafness, a blessing for the deaf treated with cochlear implantation. **© 2014 The Authors. Published by Elsevier Ltd. on behalf of IBRO. This is an open access article under the CC BY-NC-ND license (http://creativecommons.org/licenses/by-nc-nd/3.0/).**

Key words: human cochlea, spiral ganglion neurons, non-myelinated Schwann cells, laminin-β2, collagen IV, immunohistochemistry.

INTRODUCTION

Loss of auditory receptors commonly leads to a retrograde degeneration of the auditory nerve. In man, this process seems slow, incomplete (Nadol et al., 1989; Nadol and Hsu, 1991; Turner et al., 2008) and mostly involves the peripheral process or dendrite. Thus, spiral ganglion neurons (SGNs) may persist without peripheral connections to the sensory organ as monopolar or "amputated" cells with unbroken connections to the brain (Felder et al., 1997; Glueckert et al., 2005; Teufert et al., 2006; Linthicum and Fayad, 2009). There is clinical evidence that these neurons are electrically excitable even after many years of deafness (Liu et al., 2014). Pertinent cochlear implant (CI) results can be

*Corresponding authors. Address: Department of Otolaryngology, Uppsala University Hospital, SE-751 85 Uppsala, Sweden (H. Rask-Andersen).
E-mail addresses: lwoo24@gmail.com (W. Liu), Fredrik.edin@surgsci.uu.se (F. Edin), atturo@libero.it (F. Atturo), gunde.rieger@uibk.ac.at (G. Rieger), hubert.loewenheim@uni-oldenburg.de (H. Löwenheim), pascal_senn@me.com (P. Senn), michael.blumer@i-med.ac.at (M. Blumer), annelies.schrott@i-med.ac.at (A. Schrott-Fischer), helge.rask-andersen@akademiska.se (H. Rask-Andersen), rudolf.glueckert@i-med.ac.at (R. Glueckert).
† Tel: +49-441-236-398; fax: +49-441-236-260.

Abbreviations: AIS, axonal initial segment; BM, basement membrane; CI, cochlear implants; Cx43, connexin 43; ECM, extracellular matrix; EDTA, ethylene-diamine-tetra-acetic acid; IHC, immunohistochemistry; LM, light microscopy; MBP, myelin basic protein; Nav1.6, Na^+-channels; NIHL, noise-induced hearing loss; NMSC, non-myelinated Schwann cell; PBS, phosphate-buffered saline; SEM, scanning electron microscopy; SG, spiral ganglion; SGC, satellite glial cell; SGN, spiral ganglion neuron; TEM, transmission electron microscopy; type I ganglion cells, large afferent neurons innervating inner hair cell; type II ganglion cells, small afferent neurons innervating outer hair cells.

http://dx.doi.org/10.1016/j.neuroscience.2014.09.059
0306-4522/© 2014 The Authors. Published by Elsevier Ltd. on behalf of IBRO.
This is an open access article under the CC BY-NC-ND license (http://creativecommons.org/licenses/by-nc-nd/3.0/).

achieved in patients with even ossified or partly ossified cochleae where the peripheral nerve axons or dendrites can be assumed to be non-existent. Consequently, hearing impaired individuals may exhibit similar auditory profiles with divergent neuropathological changes. An appealing consequence is the current aptitude to re-sprout SGNs under relevant conditions to further improve CI results.

The essential roles played by surrounding satellite glial cells (SGCs) for the protection of neurons in various sensory ganglia have been broadly described (Pannese, 1981; Hanani et al., 2002, 2010; Hanani, 2010). We recently postulated that connexin 43 (Cx43)-mediated gap junction signaling between SGCs might play a key role and explain the unique preservation of auditory neurons following hair cell loss (Liu et al., 2014). In this paper, an additional bordering cell, named non-myelinated Schwann cell (NMSC) is described. It surrounds the pre- and post-somatic initial segments of the human type I SGNs. Its potential role in the consolidation of SGNs following dendrite atrophy is described.

EXPERIMENTAL PROCEDURES

Our study was approved by the Uppsala Ethics Review Board (No. 99398, 22/9 1999, cont., 2003, Dnr. 2013/190). Written information was given to the patient and verbal informed consent was obtained. This procedure was chosen to reduce the stress on the patient and was approved by the ethics review board. No personalized notes were made to reduce traceability and maintain patient confidentiality. The studies adhered to the rules of the Helsinki declaration. Animal presentations are from archival material in Innsbruck.

Fixation and sectioning of human cochlea

Seven cochleae belonging to seven adult patients (two male, five females; ages 40–65 years) with normal pure tone thresholds for their age were dissected out as a whole piece during petroclival meningioma surgery. In the operating room, the cochleae were immediately placed in 4% paraformaldehyde diluted with 0.1 M phosphate-buffered saline (PBS; pH 7.4). After a 24-h fixation, the fixative was replaced with 0.1 M PBS then with 0.1 M ethylene-diamine-tetra-acetic acid (Na-EDTA) solution at pH 7.2 for decalcification. After 4 weeks, the decalcified cochleae were rinsed with PBS. For frozen sections, the cochleae were embedded in Tissue-Tek (OCT Polysciences, Tokyo, Japan), rapidly frozen and sectioned at 8–10 μm using a Leica cryostat microtome. The frozen sections were collected onto gelatin/chrome-alum-coated slides and stored below −70 °C before immunohistochemistry (IHC).

Antibody and IHC

The antibody against laminin-β2 was a monoclonal antibody from the rat (catalog number #05-206, Millipore, Billerica, MA, USA; dilution 1:100). It recognizes and is specific for the β2 chain of laminin. It does not cross-react with other basement membrane (BM) components or fibronectin (FN). The type IV collagen antibody was a goat polyclonal antibody (catalog number AB769, Millipore, Billerica, MA, USA; dilution 1:10). It has less than 10% cross reactivity with collagen types I, II, III, V and VI. Myelin basic protein (MBP) antibody was a polyclonal antibody from rabbit (catalog number #AB980, Millipore, Billerica, MA, USA; dilution 1:100). The antibody against neuron-specific class III beta-tubulin (Tuj1) was a polyclonal antibody (catalog number #04-1049, Millipore, Billerica, MA, USA; dilution 1:200). Another Tubulin antibody was a monoclonal antibody from the mouse (catalog MAB1637, Millipore, Billerica, MA, USA; dilution 1:200). Antibody combination, characteristics and sources are summarized in Table 1 and more information can be found under discussion. IHC procedures on cochlear sections were described in previous publications (Liu et al., 2011, 2012). Briefly, incubation of sections on slides with solution of the antibodies was carried out under humid atmosphere at 4 °C for 20 h. After rinsing with PBS (3 × 5 min), the sections were subsequently incubated with secondary antibodies conjugated to Alexa Fluor 488 and 555 (Molecular Probes, Carlsbad, CA, USA), counter-stained with a nuclear stain DAPI (4′,6-diamidino-2-phenylindole dihydrochloride) for 5 min, rinsed with PBS (3 × 5 min) and mounted with a VECTA SHIELD (Vector Laboratories, Burlingame, CA, USA) mounting medium. The sections used for antibody control were incubated with 2% bovine serum albumin (BSA) omitting the primary antibodies. As the result of the control experiment, there was no visible staining in any structure of the cochleae.

Imaging and photography

Stained sections were investigated with an inverted fluorescence microscope (Nikon TE2000, Nikon Co., Tokyo, Japan) equipped with a spot digital camera with three filters (for emission spectra maxima at 358, 461 and 555 nm). Both microscope and camera are connected to a computer system installed with image software (NIS Element BR-3.2, Nikon) including image merging and a fluorescence intensity analyzer. For laser confocal microscopy, the same microscope was used which is equipped with laser emission and detection system with three different channels. The optical scanning and image-processing tasks were run by the program Nikon EZ-C1 (ver. 3.80) including reconstruction of Z-stack images into projections or 3D images.

Transmission electron microscopy (TEM) analysis

Two human specimens were analyzed at inner ear research laboratories in both Uppsala and Innsbruck. Tissue was rinsed in cacodylate buffer, followed by fixation with 1% osmium tetra-oxide at 4 °C for 4 h. Subsequently the cochleae were decalcified in 0.1 M Na-EDTA, pH 7.4, for 6 weeks. After decalcification, a mid-modiolar section was made and the two halves were then dehydrated in an increasing ethanol series and acetone prior to incubation in a dilution of liquid epoxy

Table 1. Antibodies used in current study

Antibody	Dilution	Poly or mono	Host	Clone	Catalog no.	Producer
Laminin-β2	1:100	Monoclonal	Rat	A5	05-206	Millipore
Type IV collagen	1:10	Polyclonal	Goat	N/A	AB769	Millipore
Type II collagen	1:50	Monoclonal	Mouse	N/A	CP18	Millipore
MBP	1:100	Polyclonal	Rabbit	N/A	AB980	Millipore
Tuj1	1:200	Monoclonal	Rabbit	N/A	04-1049	Millipore
Tuj1	1:200	Monoclonal	Mouse	N/A	MAB1637	Millipore

Poly, polyclonal antibody; mono, monoclonal antibody.

resin and acetone at a ratio of 30–70% for 3 h. The specimens were infiltrated with a mixture of Epon and acetone in equal proportions at 4 °C overnight in closed vials. The next day, a mixture of 70% epoxy resin and 30% acetone replaced the liquid for 3 h. Subsequently, tissue samples were incubated twice in 100% Epon at 4 °C for 3 h and overnight. Then, the pure epoxy resin was changed and the specimens were infiltrated with Epon in a vacuum chamber for 4 h. Sections at a thickness of 1 μm were cut on a Leica UC6 microtome, lightly stained with Toluidine Blue at 60 °C and then examined by using a light microscope. For TEM analysis, specimens were then trimmed and ultrathin sections (90-nm thickness) were acquired and transferred to pioloform F (polyvinylacetate)-coated slot grids. Staining was performed within an automated system (Leica EM Stain) with uranyl acetate (5 g/l for 30 min) and lead citrate (5 g/l for 50 min) at 25 °C. The various turns of the cochlea were analyzed and the SG from the lower basal, upper basal, lower middle, and upper middle regions was sectioned separately. Sections were viewed in a JEOL 100 SX electron microscope (Uppsala) and in Zeiss LIBRA (Institute of Zoology, Innsbruck) and Philips CM 120 (Division of Anatomy, Histology and Embryology, Innsbruck) transmission electron microscopes. In addition, we analyzed with light microscopy (LM) and TEM SGNs in a damaged region of a patient with a typical 4-kHz noise-induced hearing loss (NIHL) (Rask-Andersen et al., 2000a,b). The patient was a carpenter and had been chronically exposed to noise for 40 years. Histologically verified mono-polar type I SGNs at the 13–15-mm region were traced through 3D-reconstructions of SGNs. Serial sections were cut parallel to the central axis of the modiolus and stained with Toluidine Blue as described previously (Blumer et al., 2002). Images from 88 consecutive 1.5-μm-thick semithin sections were acquired with a Tissuefax Plus (Tissuegnostics® Austria) system using the 20× lens, converted to gray levels and aligned using the alignment module in Amira 5.5 (Visualization Sciences Group, FEI Company, Hillsboro, Oregon, USA). With the segmentation editor of the software, SGNs with their surrounding SGCs were traced manually and 3D reconstructed. All type I neurons including the relative numbers of monopolar were counted. In addition, thin sections were cut of Rosenthal's canal 10–13 mm from the round window. Sections were stained and scrutinized with TEM.

Scanning electron microscopy (SEM)

Two cochleae were used that were processed and morphologically analyzed previously (Rask-Andersen et al., 2010). Both were from middle-aged females with normal hearing. Cochleae were decalcified in 0.1 M Na-EDTA, pH 7.4, for 6 weeks. Subsequently they were washed in PBS, pH 7.4, dehydrated in graded ethanol (70, 80, 90, 95, and 100%; 10 min each), critical point-dried, and attached to aluminum stubs. Specimens were coated in a BALTECH MED020 Coating System with gold– palladium to a nominal depth of 10–12 nm and viewed in a ZEISS DSM982 Gemini field emission electron microscope operating at 5 kV. Maximal resolution at this voltage was estimated to approx. 2 nm. Digital photos were taken at 1280–1024 ppi resolution. Measurements were performed using the image analysis software Image Pro 4.5.1.29 (Media Cybernetics, Inc., MD and USA).

RESULTS

Well preserved human SGNs were obtained and verified with LM, TEM and SEM (Figs. 1, 4 and 5A). Most type I SGNs were unmyelinated and lacked expression of MBP (Figs. 1 and 2A). Instead they were surrounded by SGCs whose extracellular surface was covered by a BM (Figs. 1 and 2A–C, E, F, 3). Their cell nuclei were often crescent-like. Many type I SGNs formed clusters and were jointly surrounded by SGCs and a distinct BM (Fig. 1). The continuous BM co-expressed the β2 isoform of laminin heterotrimeric complex and collagen type IV (Figs. 2 and 3). The BM surrounded the neurons from the spiral ganglion (SG) to the nerve entry in the sensory organ (habenula perforata) and stained positive for both markers (Fig. 2D). The BM also formed a thin sheet lining the short canal into the sensory organ (habenular canal) which coalesced with the BM of the sensory epithelium. The peripheral axons (or dendrites) lost their myelin sheath beneath the inferior canal opening of the habenula perforata (Fig. 2D). Dendrites and axons of the type I SGNs were bordered by MBP-positive, myelinating Schwann cells. The pre- and post-somal segments however, were mostly bordered by unmyelinated Schwann cells (MBP-negative). The non-myelinated zones varied considerably in length but could be up to 50 microns (Fig. 2A, E). Typically, as opposed to the SGCs, the NMSCs showed rich expression of intracellular laminin-β2 and collagen IV (Figs. 2E, F, and 3). This contrasted to the SGCs that showed no such expression. The NMSCs extended to the poles of the cell soma. Their cell nuclei were often round compared to the crescent shape of the SGCs nuclei.

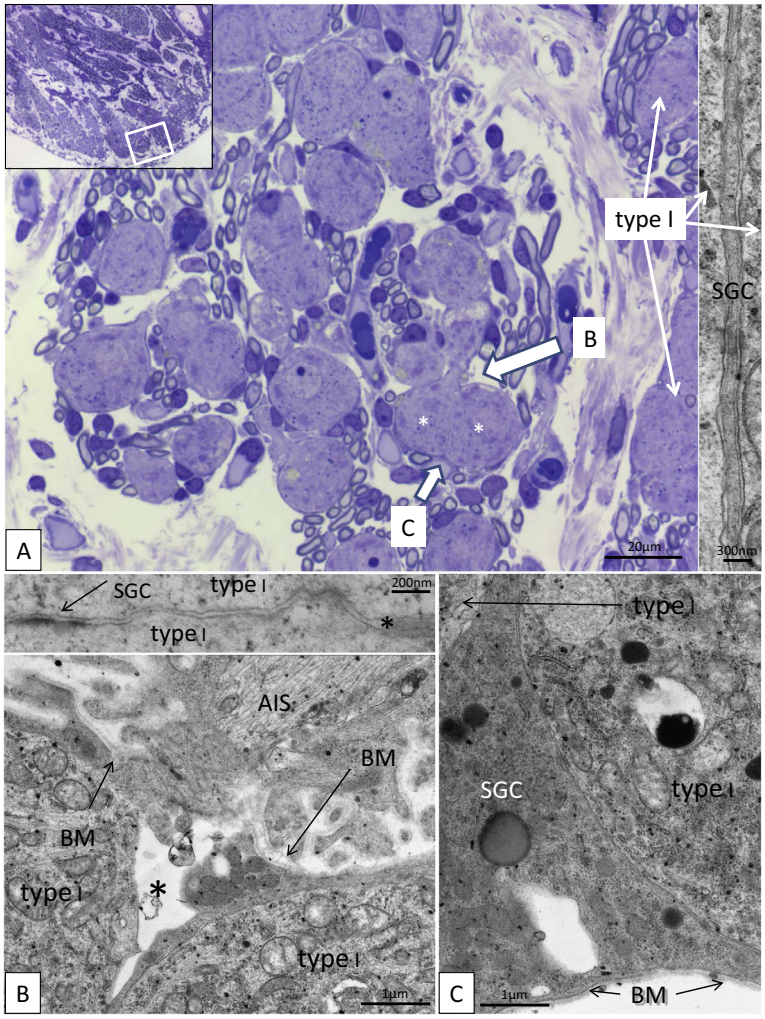

Fig. 1. Light and transmission electron microscopy of the human spiral ganglion. (A) Light microscopy of a semi-thin section from the second turn of the cochlea sectioned perpendicular to the long axis of the modiolus (upper inset). Several type I SGNs lie typically close to each other and share SGCs. Sometimes a thin rim of their cytoplasm jams itself between (middle arrow, right inset). SGCs are surrounded by a basement membrane whenever facing extra-cellular tissue. Filled arrows show AISs. Cochlea was fixed in glutaraldehyde according M&M (normal audiogram). Toluidine/osmium. Na-EDTA decalcification (section thickness approx. 1 µm). AIS, axonal initial segment. (B) TEM demonstrating AIS junction at nerve cell body in a cell cluster. There is incongruence in the basement membrane (BM) lining. Inset confirms that neural cell bodies face each other without a limiting SGC cell. The cell membranes show electron-dense specializations. (C) TEM of corresponding area shown in A (upper filled arrow). A satellite glial cell (SGC) surrounds several type I nerve bodies. The group of cells is surrounded by a basement membrane.

TEM

The SGNs were outlined by several SGCs. Sometimes groups of SGNs formed cell clusters that were jointly surrounded by SGCs (Fig. 1 and 4) and a continuous BM. Their cell membranes frequently faced each other without SGCs in between (Fig. 1A, D). Membrane specializations were seen at these areas (Fig. 1inset). The human anatomy differed greatly from the adult cat (Fig. 4D). Their type 1 neural cell bodies were always separated from each other and surrounded by a compact myelin layer. TEM of the pre- and post-somal segments of the type I SGNs showed that the NMSCs, surrounding these segments, were often extensively folded and bordered by a likewise folded BM (Fig. 4A–C). Occasionally, several NMSCs enveloped the poles of the nerve cell body and the axonal initial segment (AIS). Cytoplasm projections could extend into neighboring extracellular tissue to reach surrounding blood vessels and free connective tissue cells (Fig. 5B). The villous cell coat, sometimes gave them an ‘‘octopus-like’’ appearance (Fig. 4A). NMSCs surrounding adjacent SGNs were often physically related (Fig. 5A). At times axons narrowed at the entry zone with ‘‘valve-like’’ formations shaped by the surrounding NMSCs (Fig. 4C). Incongruence of multilayered BM were seen at the entry zones particularly in clustered type I neurons (Fig. 1B). The BM around blood vessels, Schwann cells and the basilar membrane of the organ of Corti epithelium also stained positive for the β2 isoform of laminin complex and collagen type IV.

Light microscopy 3D-reconstruction and TEM of SGNs in lesion caused by NIHL

At the circumscribed lesion approx. 10 mm from the round window extending to about 13 mm the dominant

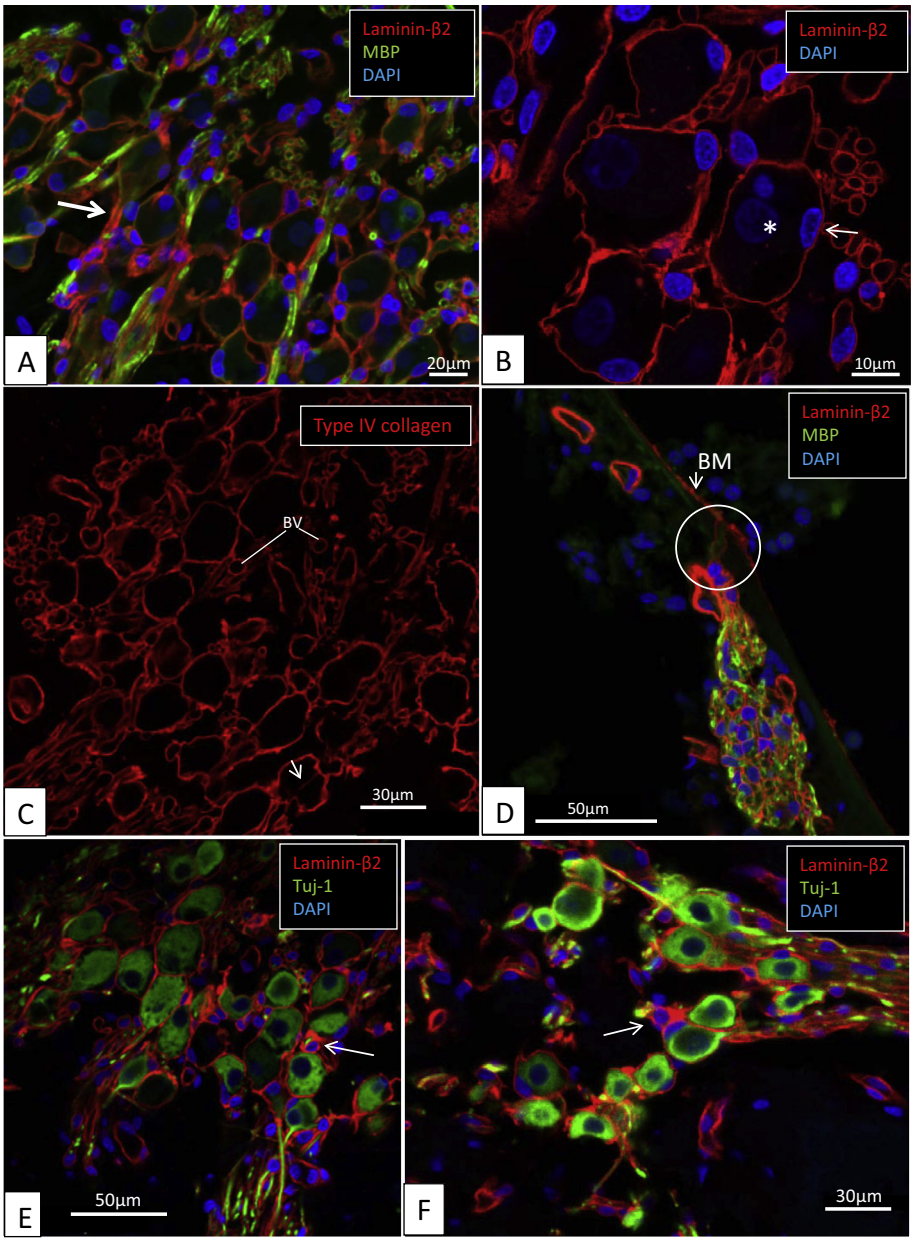

Fig. 2. Immunohistochemistry of the human spiral ganglion and habenular region. (A) Confocal microscopy demonstrating laminin-β2 and myelin basic protein (MBP) immunoreactivity in human spiral ganglion. Most type I SGNs are MBP-negative. Some non-myelinated perisomal segments show rich expression of laminin (arrow). DAPI, cell nuclei. (B) Confocal microscopy demonstrating laminin-β2 immunoreactivity of basement membrane lining the extracellular surface of the SGCs of the SGN bodies, nerve fibers and blood vessels (BV) (normal audiogram). Type I SGN cell nuclei are round and darkly stained (*) while SGC nuclei are crescent-like (arrows) and more lucent. Their cytoplasm shows no laminin expression. DAPI, nuclear staining. BV, blood vessels. (C) Confocal microscopy demonstrating collagen IV immunoreactivity of basement membrane lining the extracellular surface of the SGCs of the SGN bodies, nerve fibers and blood vessels (BV). (D) Confocal microscopy demonstrating laminin-β2 and myelin basic protein (MBP) immunoreactivity in human auditory nerves at the *habenula perforata* in the organ of Corti. Also blood vessels, Schwann cells and organ of Corti basement membrane show rich expression of laminin. Myelin is lost before neurons pass into the sensory organ. DAPI, cell nuclei. BM, basement membrane. (E) Laminin/TUJ-1 immunohistochemistry of human spiral ganglion. The perineural sheaths stain positive for laminin. Initial segments of the nerve processes generally lack myelin (large arrow). Schwann cell bodies may show rich expression of laminin (small arrow). (F) A rendered confocal microscopy stack showing laminin-β2 immunofluorescence of the human spiral ganglion. A laminin expressing NMSC is seen (thin arrow) as well as a laminin-negative SGC (thick arrow).

pathological feature was the loss of outer hair cells. The degradation of inner hair cells was less severe with a 45% loss of myelinated nerve fibers at the osseous spiral lamina (Rask-Andersen et al., 2000a,b). The number of dendrites in Rosenthal's canal was greatly reduced and only few SGNs with a peripheral process were observed (Figs.5B and 6B). 3D-reconstructions of SGNs from the patient with NIHL showed histological verified monopolar type I SGNs in 68.5% of totally 249 reconstructed SGNs. Arbitrary colored SGNs in Rosenthal's canal from the affected basal turn is shown in Fig. 5B. At TEM many neural and satellite cell bodies displayed

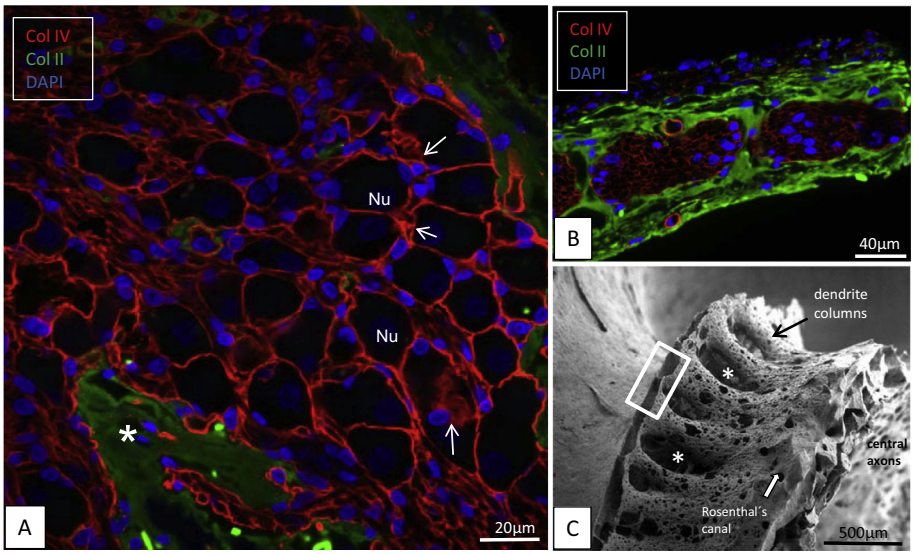

Fig. 3. Immunohistochemistry of the human spiral ganglion. (A) Confocal microscopy demonstrating collagen IV and II immunoreactivity of the spiral ganglion in the second turn of the cochlea. The basement membranes lining the outer surface of the SGCs of the SGN bodies show strong expression of collagen IV. The bony-like tissue islands express collagen II. Neural cell bodies form a mosaic and contain faintly stained nuclei (*). A few bordering cells show more intense staining for collagen IV (arrows). (B) Spiral lamina tissue expresses collagen II. The nerve fibers are surrounded by mostly myelinated Schwann cells whose basement membrane expresses collagen IV. (C) SEM of dendrite columns and initial segment of the spiral lamina in a macerated human cochlea. Between columns are bony fenestrations (*). Framed area corresponds to B.

remarkable amount of intracytoplasmic inclusion bodies. In one cell these bodies accumulated in the distal pole of the cell (Fig. 6A). Another type I cell showed a thin layer of myelin (Fig. 6B). The satellite cells covering the peripheral pole of the SGN appeared more folded than usual and the BM was often multi- or double-layered (Fig. 6C, E). There were also signs of unusual cell body interaction. Cell surfaces of SGCs showed specializations with mirrored rugosities outlined by a BM (Fig. 6D, F). Gap junctions could be observed between different SGCs (Fig. 7C, inset).

DISCUSSION

Fluorescent and confocal IHC combined with TEM of well-fixed human cochleae, seem to demonstrate a distinct type of perineural cell surrounding the initial segments of the type I SGNs. Unlike the SGCs, they showed a rich intracellular expression of laminin-β2 and collagen IV. They lacked myelin and MBP expression and we named these cells NMSCs. The nuclear shape was similar to the myelinated Schwann cells and their cell coat displayed frequently villous-like protrusions bordered by a foliated BM. These phenotypic manifestations suggest that it may represent a cell with unique functional properties (Fig. 8).

The structure of the human SGN diverges from many animal species, likely reflecting distinctive electric properties (Fig. 4D). The most noteworthy modification is the lack of compact myelin surrounding the type I neural cell bodies (Ota and Kimura, 1980; Arnold, 1982; Liu et al., 2012). Only 3.65% out of 2983 counted type I neurons were surrounded by MBP-positive SGCs in a recent study (Rattay et al., 2013). The absence of compact myelin persists along the distal and proximal segments of the axon. Another typical feature of the human SG is the cluster formations of type I neural cell bodies. The cell bodies appear in small or large groups, some even devoid of separating SGCs where inter-neural membrane specializations may occur (Rask-Andersen et al., 1997, 2000a,b; Tylstedt and Rask-Andersen, 2001). The significance of these densities has not been settled.

The temporal code in the auditory pathway is shaped by rapid spike generators initiating APs through inner hair cell (IHC) vesicular exocytosis (Rutherford et al., 2012). A strong expression of voltage-dependent Na^+-channels (Nav1.6), essential for generation of APs, is present at this location (Hossain et al., 2005). A central issue is how the APs can rapidly cross the ganglion cell body and unmyelinated axon segments in man. Spike velocity would seem to be stalled by the relatively large sized, unmyelinated type I nerve cell bodies. In the murine SG, where the type I cells are surrounded by myelinated Schwann cells, Hossain et al. (2005) found voltage-dependent Nav1.6 at multiple sites along the cochlear ganglion cells and nerve fibers for a distance of 10–15 µm. This included the afferent endings, ganglion initial segments and nodes of Ranvier. It was speculated that these spike generators offset a reduced electric propagation due to the interposing cell soma. Other authors have confirmed the localization of these channels (Fryatt et al., 2009) but have so far not been successfully localized in human tissue. SGN specializations of voltage-gated K^+ channels and voltage-gated calcium channels (VGCC α-subunits) were also described by Chen et al. (2011) and Chen and Davis (2006). Interestingly, some of these channels were also localized in surrounding Schwann cells or satellite cells, appearing differently in compact ($Ca_V2.3$, $Ca_V3.1$) and loose ($Ca_V1.2$) myelin. Voltage-gated L-type Ca^{2+} channels

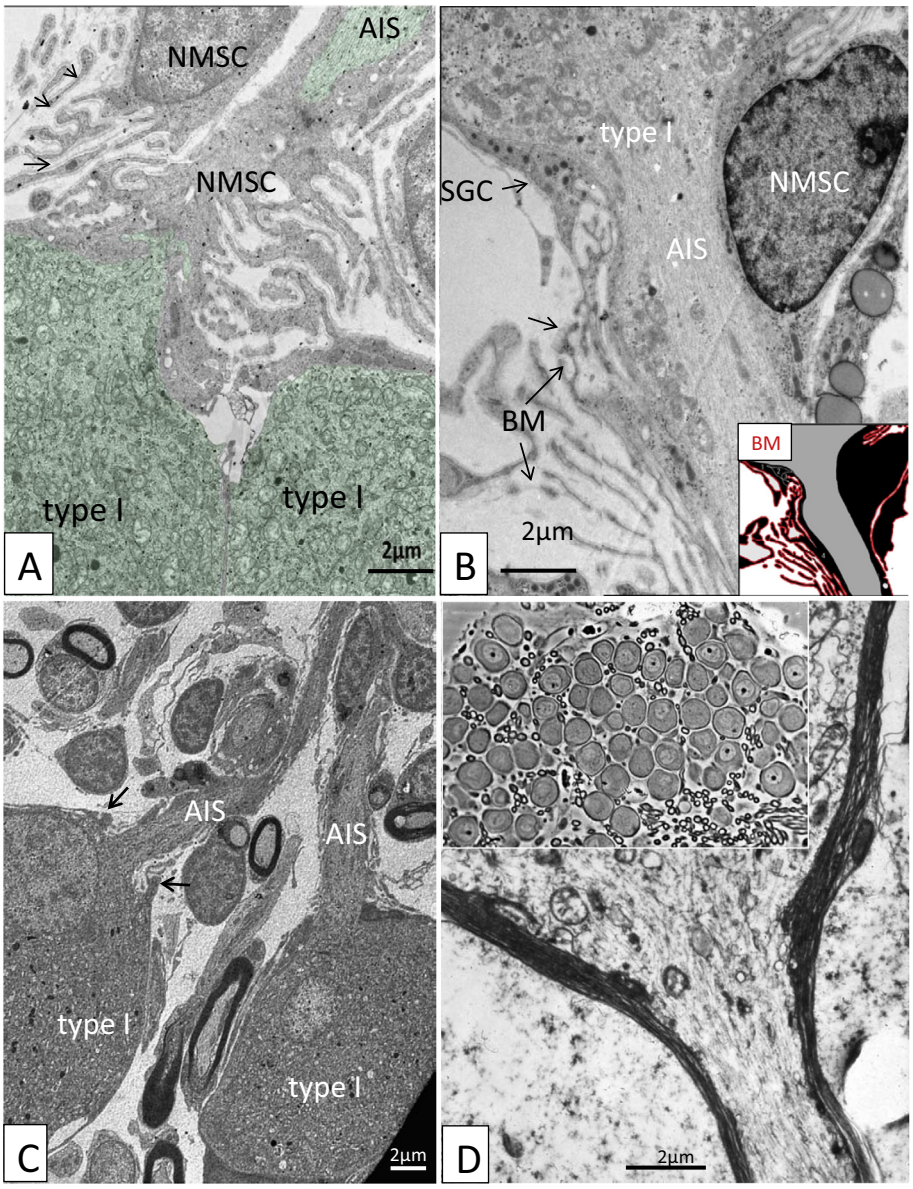

Fig. 4. Transmission electron microscopy (TEM) of SGNs in the human (A–C) and cat (D). (A) Type I SGNs (artificially stained green) at the hillock region are surrounded by several NMSCs whose cell coats are much folded and outlined by a continuous BM (arrows). AIS, axonal initial segment. (B) Extensively foliated NMSCs envelop the nerve cell pole and the axonal initial segment (AIS). A graphic delineation of the basement membrane (BM) outline (red) is shown in inset. SGC, Satellite glial cell. (C) Human type I SGNs with axonal initial segment (AIS). NMSCs surround the axonal processes. At AIS entry zone ''valve-like'' protrusions from bordering cells can be seen (arrows). (D) TEM of the hillock region in type I SGNs in the adult cat. The neural cell body is surrounded by a single myelinated Schwann cell. Inset, light microscopy of the cat SG. (For interpretation of the references to color in this figure legend, the reader is referred to the web version of this article.)

(L-VGCCs) like Cav1.2 were described in SG neurons in mice (Zuccotti et al., 2013). Thus, compensatory mechanisms may exist to uphold spike velocity and electric transmission through variously distributed spike generators. Further analyses of these channels are under way in freshly obtained surgical human cochlear tissue in our laboratory.

Thus, how and where spike generation occurs in the human auditory nerve is currently unknown. Even in patients with excellent CI outcome it could be histologically verified that most of the neurons existed in a monopolar form (Teufert et al., 2006). These ''dormant'' neurons were excitable after many years. Thus, divergent pattern of nerve decline seems to subsist in hearing-impaired individuals with comparable auditory profiles. It raises questions how and where ''amputated'' SGNs generate APs and which types of voltage-gated ion channels are involved. Electric excitation may arise at the level of the SG cell body, first segment of the central axon or the Ranvier's node. We speculate that the AIS domain surrounded by the specialized NMSCs may constitute an important site for neural excitation. Cell surface enlargement, BM filtering, multi-cellular embracement and physical interaction with surrounding blood vessels may hint that these cells could play an important role in nerve excitation in man.

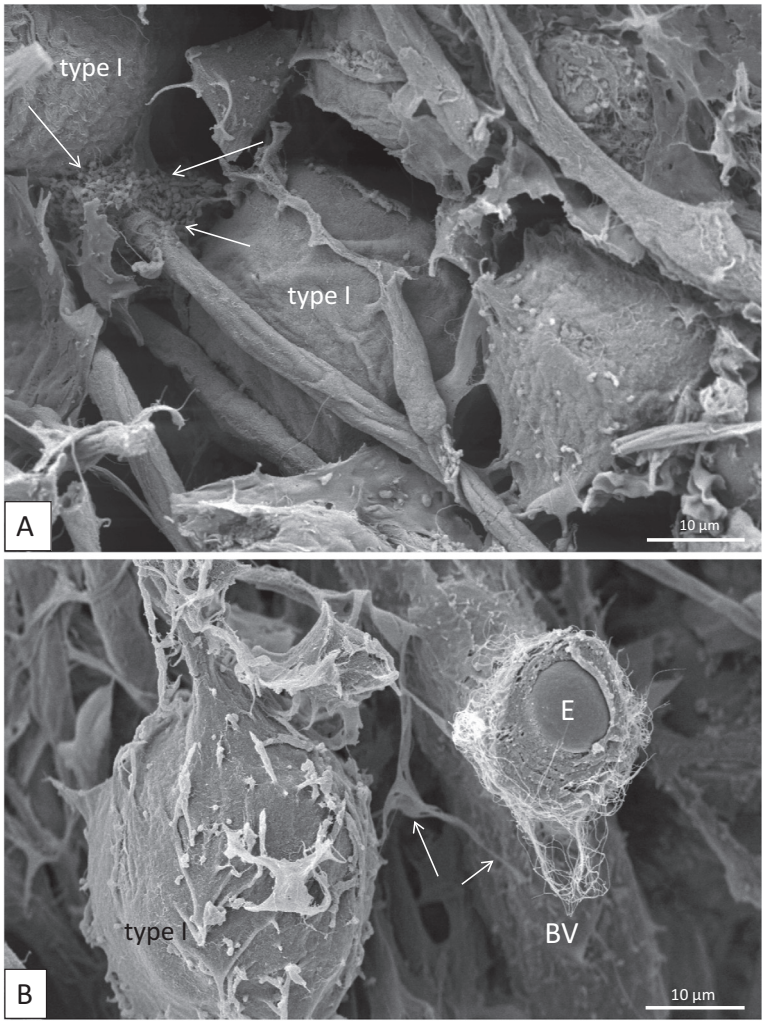

Fig. 5. SEM of human spiral ganglion. (A) Type I neurons lie close to each other. Surface coat of the bordering cells is exposed. Surface specializations (arrows) are seen near the entry zone in some cells. (B) SEM of surface coat exposing the satellite glial cells and their basement membrane. Some extensions (arrows) also reach near-by located blood vessel (BV). E, erythrocyte.

Even though a lack of compact myelin (further reducing spike conduction) appears negative for fast transmission, it may also endorse some advantages. Currents are spread and processed to several clustered neurons through cross excitation which could act synchronously to generate joint oscillations for coding complex acoustic signals such as speech. In the human SG the membrane specializations between the type 1 cells could represent membrane-associated channels that could play a decisive role of neurons' concerted action and represent channels to generate rhythms similar to those existing in the heart where hyperpolarization-activated and cyclic nucleotide-gated channels HCN1–4 (voltage-gated K^+ and cyclic nucleotide-gated channels) are known to exist (Kaupp and Seifert, 2001; Notomi and Shigemoto, 2004). These studies are under way.

The synchronization may also involve inhibitory mechanisms to sharpen the excitatory signal. This is hard to prove in the human cochlea, but an anatomic resemblance to other vertebrates' nociceptive sensory ganglion neurons where cross excitation occurs at the unmyelinated soma (Amir and Devor, 2000; Xu and Zhao, 2003) could support the existence of such local neuro-modulatory filters within the HSG.

We focused on the laminin and type IV collagen expression in BMs. Important contributions to characterize laminins and other extracellular matrix (ECM) molecules in the inner ear were performed by Rodgers et al. (2001), Takahashi and Hokunan (1992), Weinberger et al. (1999), Kalluri et al. (1998), Cosgrove et al. (1996), Swartz and Santi (1999), Tsuprun and Santi (1999, 2001), Heaney and Schulte (2003). The first comprehensive immunolocalization of ECM proteins in the human inner ear was performed by Ishiyama et al. (2009). BMs can bind a variety of cytokines and growth factors and play crucial roles during physiological remodeling or repair processes after injury. BM constituents can influence cell differentiation, proliferation and migration. We speculate that the NMSCs and their multi-cellular interaction allude to their potential for SGN repair following dendrite loss. Cx43 and the gap junction intercellular contacts between perineural cells may also be fundamental for nerve preservation (Liu et al., 2014). Up-regulations

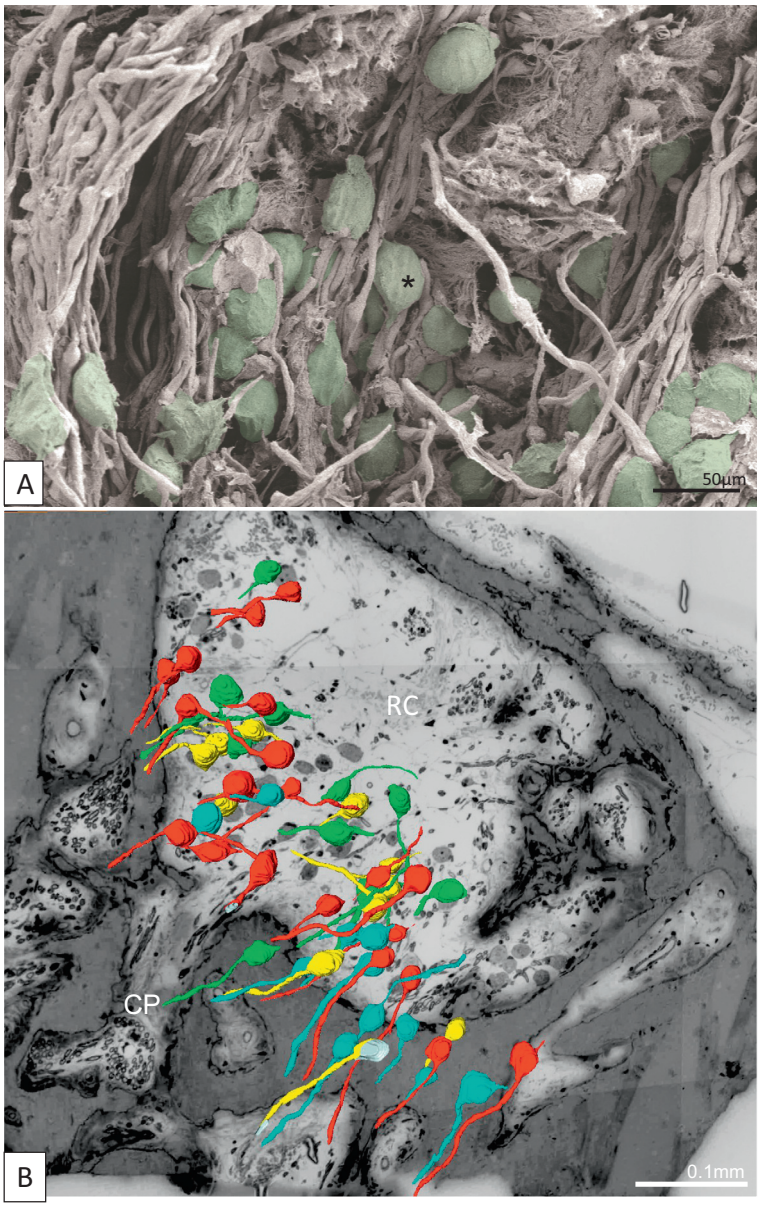

Fig. 6. SEM and 3-D reconstruction of human spiral ganglion. (A) SEM of human spiral ganglion (basal turn). Neural cell bodies have been artificially stained green. The cell coat of several neurons show longitudinal impressions (*) caused by crossing myelinated nerve fibers. (B) Light microscopy of the SGNs from a damaged region in a patient with a 4-kHz noise-induced hearing loss. Type I SGNs are depicted in arbitrary colors at the 13–15-mm region. 3D-reconstruction verified that 68.5% of totally 249 SGNs were monopolar (88 sections, 1.5-µm thick). RC, Rosenthal's canal.

of Cx43 and laminin-β2 genes were described after induced peripheral lesions in the non-neuronal dorsal root (DRG) and trigeminal ganglion cells (Beau et al., 1995; Dubovy et al., 2006). Likewise, RNA interference reducing Cx43 expression in glial cell gap junctions after nerve injury increased nociceptive behavior such as neuropathic pain (Ohara et al., 2008), a remarkable analog to cochlear tinnitus.

In an earlier TEM study, we analyzed the damaged area in a patient with typical NIHL (Rask-Andersen et al., 2000a,b). The structure of the SG supplying the lesion area appeared normal with minimal loss of large (type I) and small (type II) ganglion cells but this could not be settled with certainty due to lack of reference data. Ganglion cells could not be seen where the distal axon definitely had undergone atrophy since serial sectioning was not performed. Here, we extended the study to investigate the SGNs and prevalence of histologically verified monopolar type I SGNs at the 10–13-mm region using 3D-reconstruction of serial sections (Fig. 5B). It showed that a majority of SGNs in fact lacked dendrites. In addition, TEM demonstrated a number of changes not recognized in earlier studies of humans at similar age (Tylstedt et al., 1997; Rask-Andersen et al., 2000a,b). SGCs and even the type I cells (Fig. 6A, B, C, E) appeared more foliated with intracellular accumulation of inclusion bodies. This may be consistent with a history of increased cell degradation and dendrite atrophy. According to

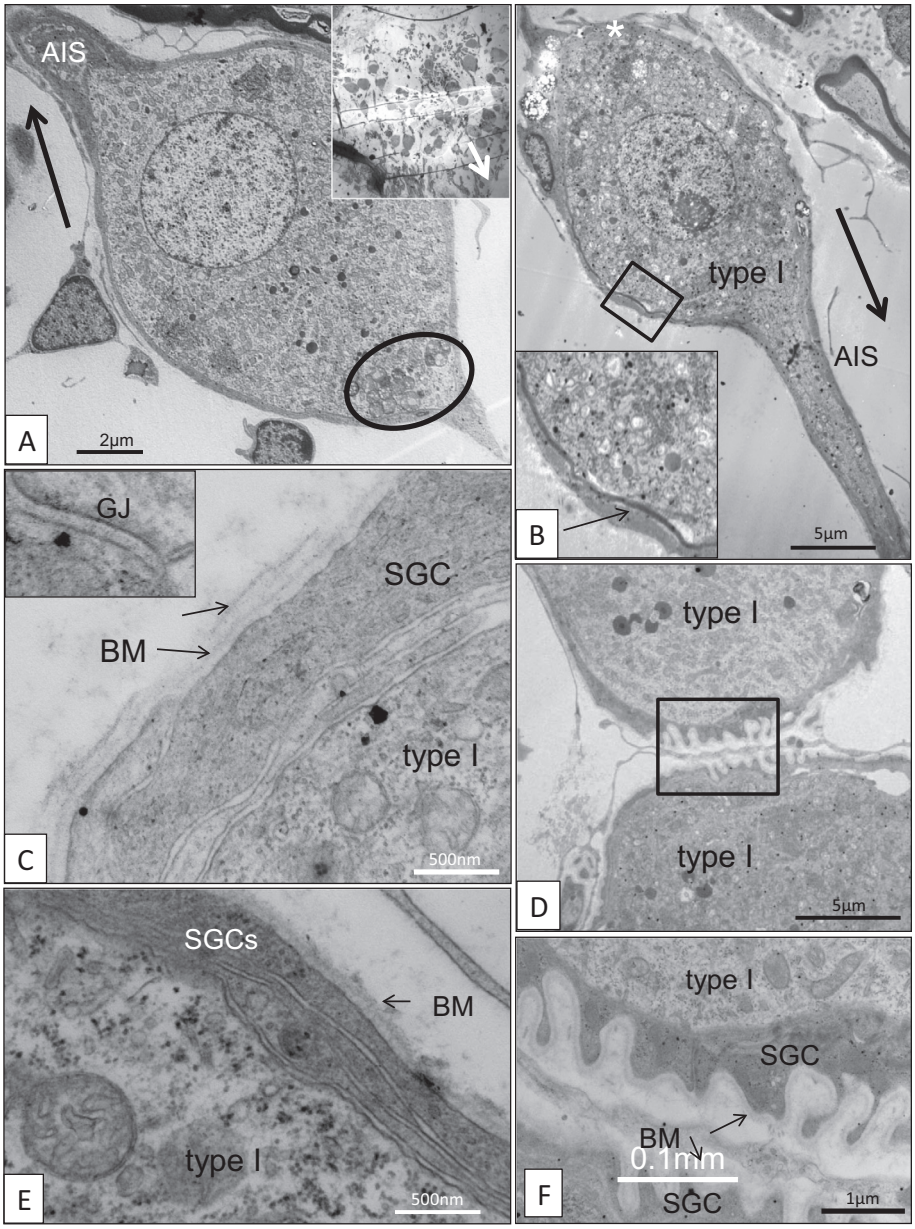

Fig. 7. TEM of SGNs in a noise-damaged area 10–13 mm from the round window corresponding to the 4–6-kHz region. (A) Type I SGN with accumulation of intracytoplasmic inclusion bodies in the distal pole. AIS, axonal initial segment. Inset shows corresponding region at low magnification. Arrows indicate central direction. (B) Type I SGN with accumulation of inclusion bodies in the SGC in the distal pole. Inset shows framed area in higher magnification. A thin rim of myelin can be seen. (C) Foliated SGCs surrounding the distal pole of a SGN. Basement membrane (BM) is double-layered. Inset shows a gap junction between SGCs. SGC, satellite glial cell. (D) SGCs showing membrane specializations surround two SGNs. Framed area is magnified in F. (E) Foliated SGCs at the distal pole of a SGN. (F) Membrane specializations between two SGNs.

Ota and Kimura (1980) 3–5% of the SGN cells are myelinated, depending on the age and status of the organ. Arnold (1982) found an increasing myelination (2%) of ganglion cells in elderly persons. The largest number of myelinated cells in our earlier studies was observed in a 60-year-old individual (approx. 2%), suggesting that myelination may increase with age. The finding of a myelinated SGN could have resulted from a degeneration process rather than the patients' age (55 years).

Loss of auditory receptors or supporting cells generally leads to a retrograde degeneration of the auditory nerve (Webster and Webster, 1981; Spoendlin, 1984; Xu et al., 1993; McFadden et al., 2004; Zilberstein et al., 2012). An eccentric condition in man is the relative resistance of the SGNs to undergo retrograde degeneration after sensory deafferentation Glueckert et al., 2005; Linthicum and Fayad, 2009; Teufert et al., 2006). Nadol et al. (1989) demonstrated in a histopathology study using multiple regression analysis that even if the number of neurons diminishes with longer duration of hearing loss and total deafness, the etiology of hearing loss was the most significant determinant of SGN count. Deterioration is slow, incomplete and generally constrained to the peripheral dendrites. Neurons persist as

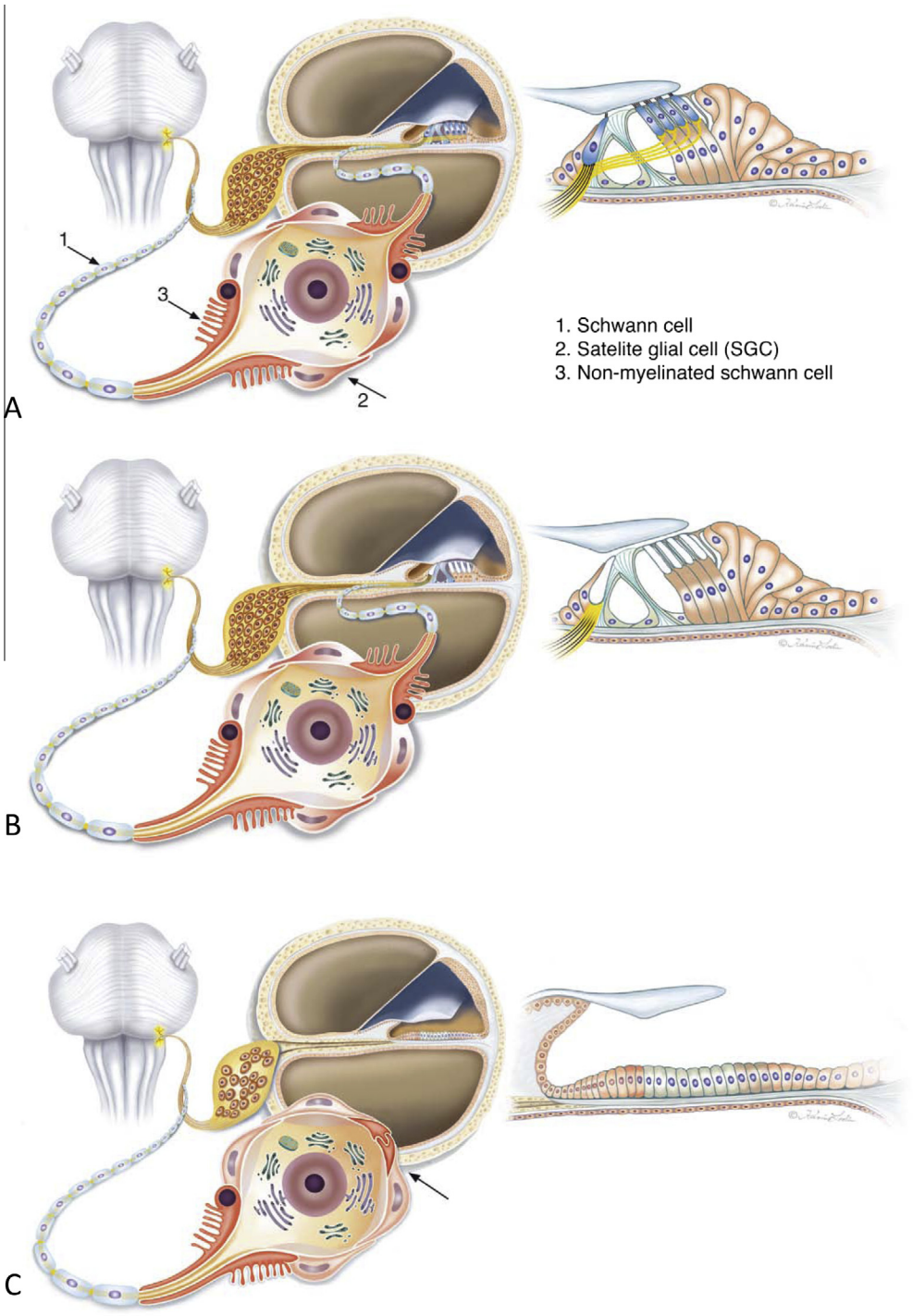

Fig. 8. Graphic showing different neuro-anatomical conditions in patients with sensorineural hearing loss. C could be prevalent in cochlear implant patients with long deafness duration. (A) Normal condition. The SGNs are surrounded by satellite glial cells (SGCs) while the pre- and post-somatic axonal segments are bordered by non-myelinated Schwann cells (NMSCs). Axons are enwrapped by regular Schwann cells. (B) Deafness is frequently caused by a loss of functional hair cells. Preservation of supporting cells can up-hold the integrity of the peripheral dendrite. (C) Loss of sensory and supporting cells may result in dendrite atrophy (Teufert et al., 2007) due to retrograde degeneration. The unmyelinated bordering cells such as SGCs and NMSCs may consolidate neurons as mono-polar or ''amputated'' cells (arrow) with unbroken connections to the brain stem. Theoretically, these neurons could be re-sprouted.

mono-polar or ''amputated'' cells with unbroken connections to the brain stem (Teufert et al., 2006; Linthicum and Fayad, 2009; Liu et al., 2014). From the following it is apparent that attempts to re-sprout an injured human SGN is an appealing strategy. Outgrowth of perikaryon projections from spinal ganglion neurons has indicated that satellite cells play a key role (Pannese et al., 1999). Axon regeneration following acute nerve section reveals that BM can form ''regenerating units'' or buds (Morris et al., 1972) with projecting growth cones. Laminin is a

potent stimulator of neurite outgrowth *in vitro* (Manthorpe et al., 1983) and BM influences differentiation of regenerating nerve terminals at synaptic sites. BM scaffolds of Schwann cells can serve as conduits for regenerating axons (Ide, 1983). Electron microscopy studies have shown that regenerating axons can grow out without Schwann cells with BM facing neural plasmalemma when treated with FGF (Fujimoto et al., 1997). In addition, laminin-sulfatide binding initiates BM assembly and enables receptor signaling in Schwann cells and fibroblasts (Li et al., 2005).

Our results are consistent with clinical experience of persisting excitable neurons in patients after long deafness duration; a blessing for those treated with CIs. Furthermore, patients with profound deafness should not be excluded from treatment with electric stimulation solely based on its duration (Lundin et al., 2014). Drug-induced re-sprouting of dendrites could also be realistic in the future to further improve functional results of cochlear implantation.

Acknowledgments—This study was supported by ALF grants from Uppsala University Hospital and Uppsala University, Sweden and by the Foundation of "Tysta Skolan", Swedish Deafness Foundation (HRF). Our research is part of the European Community 7th Framework Programme on Research, Technological Development and Demonstration. Project acronym: NANOCI. Grant agreement no: 281056 and kind private funds from Börje Runögård, Sweden. Karin Lodin is acknowledged for skilful graphical art works. Michael Blumer (cutting semi-thin ribbons), Rene Fischlechner (performing manual segmentation of neurons), Kirstian Pfaller.

REFERENCES

Arnold WJ (1982) The spiral ganglion of the newborn baby. Am J Otol 3:266–269.

Amir R, Devor M (2000) Functional cross-excitation between afferent A- and C-neurons in dorsal root ganglia. Neuroscience 95:189–195.

Beau JM, Liuzzi FJ, Depto AS, Vinik AI (1995) Up-regulation of laminin B2 gene expression in dorsal root ganglion neurons and non-neuronal cells during sciatic nerve regeneration. Exp Neurol 134:150–155.

Blumer MJ, Gahleitner P, Narzt T, Handl C, Ruthensteiner B (2002) Ribbons of semi-thin sections: an advanced method with a new type of diamond knife. J Neurosci Methods 120:11–16.

Chen WC, Xue HZ, Hsu YL, Liu Q, Patel S, Davis RL (2011) Complex distribution patterns of voltage-gated calcium channel α-subunits in the spiral ganglion. Hear Res 278:52–68.

Chen WC, Davis RL (2006) Voltage-gated and two-pore-domain potassium in murine spiral ganglion neurons. Hear Res 222:89–99.

Cosgrove D, Samuelson G, Pinnt J (1996) Immunohistochemical localization of basement membrane collagens and associated proteins in the murine cochlea. Hear Res 97:54–65.

Dubovy P, Jancalek R, Klusakova I (2006) A heterogeneous immunofluorescence staining for laminin-1 and related basal lamina molecules in the dorsal root ganglia following constriction nerve injury. Histochem Cell Biol 125:671–680.

Felder E, Kanonier G, Scholtz A, Rask-Andersen H, Schrott-Fischer A (1997) Quantitative evaluation of cochlear neurons and computer-aided three-dimensional reconstruction of spiral ganglion cells in humans with a peripheral loss of nerve fibres. Hear Res 105:183–190.

Fryatt AG, Vial C, Mulheran M, Gunthorpe MJ, Grubb BD (2009) Voltage-gated sodium channel expression in rat spiral ganglion neurons. Mol Cell Neurosci 42:399–407.

Fujimoto E, Mizoguchi A, Hanada K, Yajima M, Ide C (1997) Basic fibroblast growth factor promotes extension of regenerating axons of peripheral nerve. In vivo experiments using a Schwann cell basal lamina tube model. J Neurocytol 26:511–528.

Glueckert R, Pfaller K, Kinnefors A, Rask-Andersen H, Schrott-Fischer A (2005) The human spiral ganglion: new insights into ultrastructure, survival rate and implications for cochlear implants. Audiol Neurootol 10:258–273.

Hanani M, Huang TY, Cherkas PS, Ledda M, Pannese E (2002) Glial cell plasticity in sensory ganglia induced by nerve damage. Neuroscience 114:279–283.

Hanani M, Caspi A, Belzer V (2010) Peripheral inflammation augments gap junction-mediated coupling among satellite glial cells in mouse sympathetic ganglia. Neuron Glia Biol 6:85–89.

Heaney DL, Schulte BA (2003) Dystroglycan expression in the mouse cochlea. Hear Res 177:12–20.

Hanani M (2010) Satellite glial cells: more than just 'rings around the neuron'. Neuron Glia Biol 6:1–2.

Hossain WA, Antic SD, Yang Y, Rasband MN, Morest DK (2005) Where Is the spike generator of the cochlear nerve? voltage-gated sodium channels in the mouse cochlea. J Neurosci 25:6857–6868.

Ide C (1983) Nerve regeneration and Schwann cell basal lamina: observations of the long-term regeneration. Arch Histol Jpn 46:243–257.

Ishiyama A, Mowry SE, Lopez IA, Ishiyama G (2009) Immunohistochemical distribution of basement membrane proteins in the human inner ear from older subjects. Hear Res 254:1–14.

Kalluri R, Gattone 2nd VH, Hudson BG (1998) Identification and localization of type IV collagen chains in the inner ear cochlea. Connect Tissue Res 37:143–150.

Kaupp UB, Seifert R (2001) Molecular diversity of pacemaker ion channels. Annu Rev Physiol 63:235–257. Review.

Li S, Liquari P, McKee KK, Harrison D, Patel R, Lee S, Yurchenco PD (2005) Laminin-sulfatide binding initiates basement membrane assembly and enables receptor signaling in Schwann cells and fibroblasts. J Cell Biol 169:179–189.

Linthicum Jr FH, Fayad JN (2009) Spiral ganglion cell loss is unrelated to segmental cochlear sensory system degeneration in humans. Otol Neurotol 30:418–422.

Liu W, Bostrom M, Kinnefors A, Linthicum Jr FH, Rask-Andersen H (2012) Expression of myelin basic protein in the human auditory nerve – an immunohistochemical and comparative study. Auris Nasus Larynx 39:18–24.

Liu W, Glueckert R, Linthicum FH, Rieger G, Blumer M, Bitsche M, Pechriggl E, Rask-Andersen H, Schrott-Fischer A (2014) Possible role of gap junction intercellular channels and connexin 43 in satellite glial cells (SGCs) for preservation of human spiral ganglion neurons A comparative study with clinical implications. Cell Tissue Res 355:267–278.

Liu W, Kinnefors A, Boström M, Rask-Andersen H (2011) Expression of TrkB and BDNF in human cochlea—an immunohistochemical study. Cell Tissue Res 345:213–221.

Lundin K, Stillesjö F, Rask-Andersen H (2014) Experiences and results from cochlear implantation in patients with long duration of deafness. Audiol Neurotol Extra 4:46–55.

Manthorpe ME, Engvall E, Ruoslahti F, Longo G, Davis G, Varon S (1983) Laminin promotes neuritic regeneration from cultured peripheral and central neurons. J Cell Biol 97:1882–1890.

McFadden SL, Ding D, Jiang H, Salvi RJ (2004) Time course of efferent fiber and spiral ganglion cell degeneration following complete hair cell loss in the chinchilla. Brain Res 997:40–51.

Morris JH, Hudson AR, Weddell G (1972) A study of degeneration and regeneration in the divided rat sciatic nerve based on electron microscopy. Z Zellforsch Mikrosk Anat 124:103–130.

Nadol Jr JB, Young YS, Glynn RJ (1989) Survival of spiral ganglion cells in profound sensorineural hearing loss: implications for cochlear implantation. Ann Otol 98:411–416.
Nadol Jr JB, Hsu WC (1991) Histopathologic correlation of spiral ganglion cell count and new bone formation in the cochlea following meningogenic labyrinthitis and deafness. Ann Otol Rhinol Laryngol 100:712–716.
Notomi T, Shigemoto R (2004) Immunohistochemical localization of Ih channel subunits, HCN1-4, in the rat brain. J Comp Neurol 471:241–276.
Ohara PT, Vit JP, Bhargava A, Jasmin L (2008) Evidence for a role of connexin 43 in trigeminal pain using RNA interference in vivo. J Neurophysiol 100:3064–3073.
Ota CY, Kimura RS (1980) Ultrastructural study of the human spiral ganglion. Acta Otolaryngol 9:53–62.
Pannese E (1981) The satellite cells of the sensory ganglia. Adv Anat Embryol Cell Biol 65:1–111.
Pannese E, Procacci P, Berti E, Ledda M (1999) The perikaryal surface of spinal ganglion neurons: differences between domains in contact with satellite cells and in contact with the extracellular matrix. Anat Embryol (Berl) 199:199–206.
Rask-Andersen H, Tylstedt S, Kinnefors A, Schrott-Fischer A (1997) Nerve fibre interaction with large ganglion cells in the human spiral ganglion. A TEM study. Auris Nasus Larynx 24:1–11.
Rask-Andersen H, Tylstedt S, Kinnefors A, Illing R (2000a) Synapses on human spiral ganglion cells: a transmission electron microscopy and immunohistochemical study. Hear Res 141:1–11.
Rask-Andersen H, Ekvall L, Scholtz A, Schrott-Fischer A (2000b) Structural/audiometric correlations in a human inner ear with noise-induced hearing loss. Hear Res 141:129–139.
Rask-Andersen H, Liu W, Linthicum F (2010) Ganglion cell and 'dendrite' populations in electric acoustic stimulation ears. Adv Otorhinolaryngol 67:14–27.
Rattay F, Potrusil T, Wenger C, Wise AK, Glueckert R, Schrott-Fischer A (2013) Impact of morphometry, myelinization and synaptic current strength on spike conduction in human and cat spiral ganglion neurons. PLoS One 8:8–11.
Rodgers KD, Barritt L, Miner JH, Cosgrove D (2001) The laminins in the murine inner ear: developmental transitions and expression in cochlear basement membranes. Hear Res 158:39–50.
Rutherford MA, Chapochnikov NM, Moser T (2012) Spike encoding of neurotransmitter release timing by spiral ganglion neurons of the cochlea. J Neurosci 32:4773–4789.
Spoendlin H (1984) Factors inducing retrograde degeneration of the cochlear nerve. Ann Otol Suppl 112:93. No. 4 part 2.
Swartz DJ, Santi PA (1999) Immunolocalization of tenascin in the chinchilla inner ear. Hear Res 130:108–114.
Takahashi M, Hokunan K (1992) Localization of type IV collagen and laminin in the guinea pig inner ear. Ann Otol Suppl 157:58–62.
Teufert KB, Linthicum Jr FH, Connell SS (2006) The effect of organ of Corti loss on ganglion cell survival in humans. Otol Neurotol 27:1146–1151.
Tsuprun V, Santi P (1999) Ultrastructure and immunohistochemical identification of the extracellular matrix of the chinchilla cochlea. Hear Res 129:35–49.
Tsuprun V, Santi P (2001) Proteoglycan arrays in the cochlear basement membrane. Hear Res 157:65–76.
Turner C, Reiss L, Gantz B (2008) Combined acoustic and electric hearing preserving residual acoustic hearing. Hear Res 242:164–171.
Tylstedt S, Kinnefors A, Rask-Andersen H (1997) Neural interaction in the human spiral ganglion: a TEM study. Acta Otolaryngol 117:505–512.
Tylstedt S, Rask-Andersen H (2001) A 3-D model of membrane specializations between human auditory spiral ganglion cells. J Neurocytol 30:465–473.
Webster M, Webster DB (1981) Spiral ganglion neuron loss following organ of Corti loss: a quantitative study. Brain Res 212:17–30.
Weinberger DG, ten Cate W-C, Lautermann J, Baethmann M (1999) Localization of laminin isoforms in the guinea pig cochlea. Laryngoscope 109:2001–2004.
Xu SA, Shepherd RK, Chen Y, Clark GM (1993) Profound hearing loss in the cat following the single co-administration of kanamycin and ethacrynic acid. Hear Res 70:205–215.
Xu GY, Zhao ZQ (2003) Cross-inhibition of mechanoreceptive inputs in dorsal root ganglia of peripheral inflammatory cats. Brain Res 970:188–194.
Zilberstein Y, Liberman MC, Corfas G (2012) Inner hair cells are not required for survival of spiral ganglion neurons in the adult cochlea. J Neurosci 32:405–410.
Zuccotti A, Lee SC, Campanelli D, Singer W, Satheesh SV, Patriarchi T, Geisler HS, Köpschall I, Rohbock K, Nothwang HG, Hu J, Hell JW, Schimmang T, Rüttiger L, Knipper M (2013) L-type CaV1.2 deletion in the cochlea but not in the brainstem reduces noise vulnerability: implication for CaV1.2-mediated control of cochlear. Front Mol Neurosci 9:6–20.

(Accepted 25 September 2014)
(Available online 12 October 2014)